Downloaded from orbit.dtu.dk on: Dec 18, 2017

Technical University of Denmark

Calibration of a spinner anemometer for wind speed measurements

Demurtas, Giorgio; Friis Pedersen, Troels; Zahle, Frederik

Published in:
Wind Energy

Link to article, DOI:
10.1002/we.1965

Publication date:
2016

Document Version
Peer reviewed version

Link back to DTU Orbit

Citation (APA):
Demurtas, G., Friis Pedersen, T., & Zahle, F. (2016). Calibration of a spinner anemometer for wind speed measurements. Wind Energy, 19(11), 2003–2021. DOI: 10.1002/we.1965

DTU Library
Technical Information Center of Denmark

General rights
Copyright and moral rights for the publications made accessible in the public portal are retained by the authors and/or other copyright owners and it is a condition of accessing publications that users recognise and abide by the legal requirements associated with these rights.

- Users may download and print one copy of any publication from the public portal for the purpose of private study or research.
- You may not further distribute the material or use it for any profit-making activity or commercial gain
- You may freely distribute the URL identifying the publication in the public portal

If you believe that this document breaches copyright please contact us providing details, and we will remove access to the work immediately and investigate your claim.

WIND ENERGY
Wind Energ. 0000; **00**:1–21
DOI: 10.1002/we

RESEARCH ARTICLE

Calibration of a spinner anemometer for wind speed measurements

Giorgio Demurtas, Troels Friis Pedersen and Frederik Zahle

Technical University of Denmark, Frederiksborgvej 399, P.O. Box 49, 4000 Roskilde, Denmark.

ABSTRACT

The power curve of a wind turbine can be measured, according to IEC 61400-12-2 with a nacelle mounted anemometer. Typically, a sonic anemometer or a cup anemometer and a wind vane are mounted on the back of the nacelle roof. Another option to measure the wind experienced by the wind turbine is to use a spinner anemometer.
The measurement principle of the spinner anemometer is based on the flow distortion caused by the wind turbine spinner. The flow on the spinner surface is measured by means of three 1D sonic sensors mounted on the spinner and a conversion algorithm to convert the wind velocity components measured by the three sonic sensors to: horizontal wind speed, yaw misalignment and flow inclination angle. The algorithm utilizes two calibration constants that are specific to the spinner shape, blade root design and to the mounting positions of the sonic sensors on the spinner.
The present analysis describes methods to determine the calibration constant related to wind speed measurements. The first and preferred method is based on the definition of the calibration constant and uses wind speed measurements during the stopped condition of the wind turbine. In addition to this preferred method, two alternative methods that did not require the turbine to be stopped were investigated: one used relatively high wind speed measurements during normal operation of the wind turbine, while the other one used a CFD simulation of the flow over the spinner. The method that entails stopping the turbine in good wind conditions showed the best results and is recommended for the stall regulated wind turbine we have tested. The evaluation of uncertainty was not included in the present analysis. Copyright © 0000 John Wiley & Sons, Ltd.

KEYWORDS

anemometer; spinner anemometer; spinner anemometer calibration; iSpin; nacelle anemometry; calibration; wind speed;

Correspondence
DTU, Wind Energy Department, Building 118, Frederiksborgvej 399, P.O. Box 49, 4000 Roskilde, Denmark.
E-mail: giod@dtu.dk

Contract/grant sponsor
This work was performed under the EUDP-2012-I project: iSpin (J.nr 64012-0107)

Received . . .

Copyright © 0000 John Wiley & Sons, Ltd.

Prepared using weauth.cls [Version: 2010/06/17 v1.00]

LIST OF SYMBOLS

V_1 Velocity component of the wind speed along sensor path 1;
V_2 Velocity component of the wind speed along sensor path 2;
V_3 Velocity component of the wind speed along sensor path 3;
V_{ave} Average of V_1, V_2, V_3.
U_d Wind speed vector modulus measured by the spinner anemometer prior to calibration;
U Wind speed vector modulus at the spinner anemometer (reference value to calibrate U_d, equal to the free wind speed vector modulus in stopped conditions or conditions of null rotor induction);
U_{hor} Horizontal wind speed component measured with the spinner anemometer (calibrated value);
$U_{hor,d}$ Horizontal wind speed component measured with the spinner anemometer (non calibrated value);
$U_{hor,d,c}$ Horizontal wind speed component measured with the spinner anemometer (corrected with F_α but not F_1);
U_α Wind velocity component in the plane perpendicular to the shaft axis x_s.
U_x Wind velocity component along x;
U_y Wind velocity component along y;
U_z Wind velocity component along z;
$U_{x,n}$ Wind velocity component along x_n;
$U_{y,n}$ Wind velocity component along y_n;
$U_{z,n}$ Vertical wind velocity component, along z_n;
$U_{x,s}$ Wind velocity component along x_s;
$U_{y,s}$ Wind velocity component along y_s;
$U_{z,s}$ Wind velocity component along z_s;
δ Shaft tilt angle;
β Flow inclination angle (positive when upwards);
γ Yaw misalignment;
α Inflow angle with respect to the shaft axis;
α_d Inflow angle with respect to the shaft axis measured by the spinner anemometer prior to calibration;
ϕ Rotor position (equal to zero when sonic sensor one is at top position, positive clockwise);
θ Azimuth position of flow stagnation point on spinner (relative to sonic sensor 1);
θ_{yaw} Yaw direction referred to geographical coordinate system;
θ_{dir} Wind direction referred to geographical coordinate system;
k_1 Calibration constant mainly related to wind speed calibration;
k_α Calibration constant related to angle calibration;
k_2 Calibration constant mainly related to angle calibration (equal to $k_\alpha \cdot k_1$);
F_1 Calibration correction factor mainly related to wind speed calibration;
F_α Calibration correction factor related to angle calibration;
F_2 Calibration correction factor mainly related to angle calibration (equal to $F_\alpha \cdot F_1$);
σ Standard deviation;
N Number of measurements;
I Rotor induction, calculated as $I = (U_{mm} - U_{hor})/U_{mm}$.
U_{mm} Horizontal wind speed component (free wind speed measured with the met-mast);
U_{free} Horizontal wind speed component measured with the spinner anemometer and corrected with the nacelle transfer function to free wind speed;
$U_{N,i}$ Nacelle wind speed average value in bin i of the Nacelle Transfer Function;
$U_{F,i}$ Free wind speed average value in bin i of the Nacelle Transfer Function.

LIST OF ABBREVIATIONS

s.a. Spinner Anemometer;
NTF Nacelle Transfer Function;
NPC Nacelle Power Curve;
PC Power Curve
IEC International Electrotechnical Commission;
rpm Revolutions per minute.

Wind Energ. 0000; **00**:1–21 © 0000 John Wiley & Sons, Ltd.
DOI: 10.1002/we
Prepared using weauth.cls

1. INTRODUCTION

The spinner anemometer [1] can be used to measure the inflow wind speed to a wind turbine and to measure its power performance. For this last purpose, spinner anemometers need to be calibrated similarly to nacelle cup anemometers. Previous research [2] [3] described problems related to cup anemometers and wind vanes, or 2D sonic anemometers, mounted on top of the nacelle. The flow distortion caused by the blade roots and nacelle affects even state of the art nacelle anemometry instruments. This flow distortion is normally corrected for in the wind turbine control system. However, corrections in the controller might not take all situations into account, for example when the wake swirl from upstream wind turbines introduces upwards and downwards flow on the nacelle [9]. Such corrections are not required for a spinner anemometer, which is not affected by blade wakes since it measures the wind upstream of the rotor (figure 1). The measurement principle used by the spinner anemometer is actually based on the flow distortion created by the spinner. Due to the size of a modern wind turbine spinner and imperfections of the spinner shape, such as poor rotational symmetry, it is challenging to mount the sensors equally distant from the spinner center, and spaced 120°. These challenges in the spinner anemometer mounting could be easily solved in the future by integrating the sensor mounting holes in the spinner mould, and by improving the spinner quality control during manufacture of the spinner.

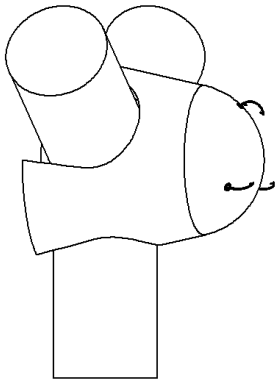

Figure 1. A drawing showing a spinner anemometer with three sonic sensors [5]

The calibration of a spinner anemometer accounts for the shape of the spinner, mounting position of the sonic sensors and characteristics of the sensors, while the rotor induction is accounted for with the Nacelle Transfer Function (NTF) as defined in IEC 61400-12-2 [11]. It is important to keep the wind speed calibration separate from the NTF, so that changes due to the spinner anemometer (mounting position of the sonic sensors, spinner geometry) can be accounted for with a new calibration only, whereas changes in the wind turbine control system or blades can be accounted with a new NTF only.

This separation between calibration of the spinner anemometer and the NTF of the wind turbine allows for direct use of the calibration values k_1 and k_2 determined on one turbine for several other turbines with the same spinner shape, verifying the sensors mounting positions with photos and estimating an additional uncertainty associated with the mounting position. The NTF determined on the first turbine can then be used on all other turbines to measure the power curve according to [11], as long as the induction at the center of the rotor can be assumed unchanged.

The calibration of the spinner anemometer requires five steps, see figure 2. Depending on the intended use of the spinner anemometer it is not required to execute all the steps. See table I for clarification of which steps are required depending on the intended use of the spinner anemometer.

The zero wind calibration is executed by the manufacturer, see figure 2. If power performance measurements are performed according to [11] the sonic sensors must be individually calibrated in a wind tunnel. The internal calibration (see figure 2) is an automatic calibration made during normal operation of the wind turbine soon after the installation of the spinner anemometer. The calibration for inflow angle measurements is then made at a stand still [5]. A practical guide [4] describes in more detail the execution of each calibration step.

The present article describes the calibration for wind speed measurements (fifth step in figure 2) and gives a demonstration of the use of the NTF to calculate the free wind starting from spinner anemometer measurements. The ability to calculate the free wind based on spinner anemometer measurements is useful for power performance measurements. The correlation between wind turbine power and wind speed was found to be higher for the spinner anemometer than for a nacelle roof anemometer or a met-mast. This allows to reduce the averaging time (which is typically 10 minutes). The Fastwind project report [6] found that a power curve made with 2 minute averaging time was very close to the one made with 10 minute averages, and was ranging up to a much higher wind speed.

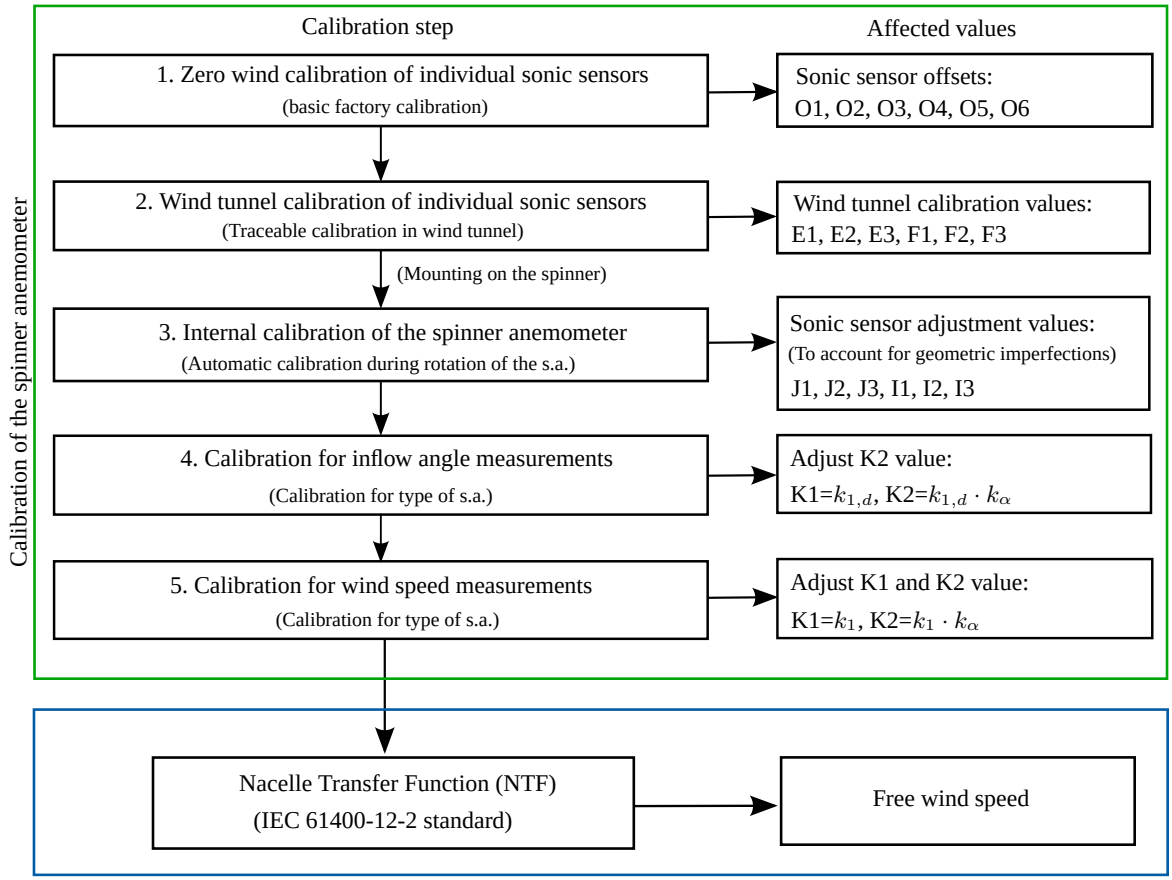

Figure 2. Overview of the sequence of steps necessary to calibrate a spinner anemometer (from [4]). Elements enclosed in the green contour are related to the calibration, while those in the blue box refer to the Nacelle Transfer Function needed to calculate the free wind speed as described in the IEC standard [11]. The boxes on the right side within the green box specify which parameters of the spinner anemometer need to be updated.

Calibration steps 1 to 5	Wind speed for power performance measurement according to IEC 61400-12-2	Wind speed for operation of the wind turbine	Yaw misalignment for operation of the wind turbine.
1) Zero wind calibration	Required	Required	Required
2) Wind tunnel calibration	Required		
3) Internal calibration	Required *	Required *	Required *
4) Calibration for inflow angle measurement	Required	Required	Required
5) Calibration for wind speed measurements	Required	Required	
Nacelle Transfer Function (NTF)	Required		

* Only required to average out spinner and sonic sensor installation imperfections over a full rotation. For 10 min. average measurements this calibration has no effect, while it has an effect on turbulence measurements and non averaged measurements.

Table I. Indication of which calibration steps should be performed depending on the intended use of the spinner anemometer.

For calibration purposes, the horizontal wind speed $U_{hor,d}$ measured by the (non calibrated) spinner anemometer is related to a met-mast hub-height wind speed measurement U_{mm} by means of the default $k_{1,d}$ constant.

Wind Energ. 0000; **00**:1–21 © 0000 John Wiley & Sons, Ltd.
DOI: 10.1002/we
Prepared using weauth.cls

The relationship between $U_{hor,d}$ and U_{mm} is linear as long as the angular measurements are calibrated with the correct k_α (fourth step in figure 2, see [5]). For this reason it is best to set the calibration value for inflow angle measurements in the spinner anemometer conversion box before the wind speed calibration is performed.

The experimental set-up used for the present article is a Nordtank 500 kW wind turbine located at DTU Risø campus, Denmark, and a met-mast with hub height measurements of wind speed and wind direction.

The next two sections describe the coordinate system and the conversion algorithm (see [5] for a detailed explanation of the conversion algorithm).

2. COORDINATE SYSTEM

The coordinate systems for transforming the spinner anemometer parameters are shown in figure 3. The inflow angle α, that is not shown, is the angle between the shaft axis and the vector of the inflow wind speed U. The yaw misalignment γ is defined as $\gamma = \theta_{dir} - \theta_{yaw}$.

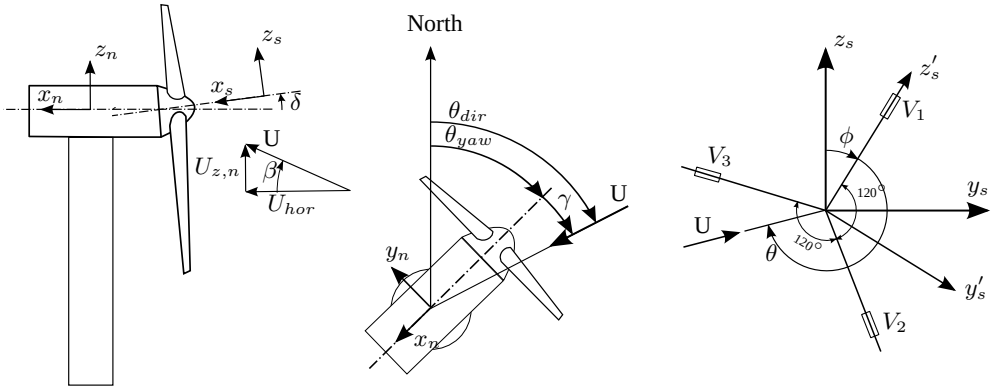

(a) Side view **(b)** Top view **(c)** Front view along the shaft axis

Figure 3. Coordinate systems and definition of angles: rotating spinner coordinate system (x_s', y_s', z_s'), non-rotating shaft coordinate system (x_s, y_s, z_s), fixed nacelle coordinate system (x_n, y_n, z_n), yaw direction yaw,yaw error γ, flow inclination angle β, tilt angle δ, azimuth position of flow stagnation point on spinner θ (relative to sonic sensor 1), rotor azimuth position ϕ (position of sonic sensor 1 relative to vertical).

3. OVERVIEW OF THE SPINNER ANEMOMETER CONVERSION ALGORITHM

A detailed description of the conversion algorithm is given in [5]. Here we show the equations in the order they are used in the conversion. The measurement principle of the spinner anemometer is based on the flow over the spinner, which is measured close to the spinner surface with three wind velocity sensors. 1D sonic sensors are used typically with a sensor path placed approximately 10 cm above the spinner surface. Accelerometers integrated in the sonic sensors are used to calculate the rotor position.

The fundamental mathematical model (equations 1, 2 and 3) assumes that the flow is uniform in a section upstream of the spinner in a circle of 0.5 m in diameter, and that the wind velocity component measured by the sensors (V_1, V_2, V_3) are sinusoidal as a function of the position θ of the flow stagnation point for a constant inflow wind speed U.

$$V_1 = U\left(k_1 \cos\alpha - k_2 \sin\alpha \cos\theta\right) \tag{1}$$

$$V_2 = U\left(k_1 \cos\alpha - k_2 \sin\alpha \cos\left(\theta - \frac{2\pi}{3}\right)\right) \tag{2}$$

$$V_3 = U\left(k_1 \cos\alpha - k_2 \sin\alpha \cos\left(\theta - \frac{4\pi}{3}\right)\right) \tag{3}$$

The spinner anemometer conversion algorithm transforms the sonic sensor wind velocity components V_1, V_2 and V_3 and the rotor azimuth position ϕ measurements into the spinner anemometer output parameters: horizontal wind speed U_{hor}, yaw misalignment γ and flow inclination angle β. This transformation (section 3.1 and Figure 4) is called direct transformation and runs inside the spinner anemometer conversion box.

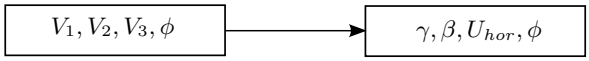

Figure 4. Direct transformation from sonic sensor wind speeds to spinner anemometer parameters.

The inverse transformation (section 3.2) transforms the output of the spinner anemometer into the input values V_1, V_2 and V_3. This is needed to post-calibrate measurements that were acquired with certain (default) calibration constant to new calibration constants, as described in section 3.3.

3.1. Direct transformation

The mathematical expressions of the conversion algorithm implemented in the spinner anemometer are:

$$\alpha = \arctan\left(\frac{k_1\sqrt{3(V_1 - V_{ave})^2 + (V_2 - V_3)^2}}{\sqrt{3}k_2 V_{ave}}\right) \quad (4)$$

$$V_{ave} = \frac{1}{3}(V_1 + V_2 + V_3) \quad (5)$$

$$U = \frac{V_{ave}}{k_1 \cos\alpha} \quad (6)$$

$$V_1 < V_{ave} : \theta = \arctan\frac{(V_2 - V_3)}{\sqrt{3}(V_1 - V_{ave})} \quad (7)$$

$$V_1 \geq V_{ave} : \theta = \arctan\frac{(V_2 - V_3)}{\sqrt{3}(V_1 - V_{ave})} + \pi \quad (8)$$

$$U_{x,s} = U\cos(\alpha) \quad (9)$$

$$U_\alpha = U\sin(\alpha) \quad (10)$$

$$U_{y,s} = -U_\alpha \sin(\phi + \theta) \quad (11)$$

$$U_{z,s} = -U_\alpha \cos(\phi + \theta) \quad (12)$$

$$U_x = U_{x,s}\cos(\delta) + U_{z,s}\sin(\delta) \quad (13)$$

$$U_y = U_{y,s} \quad (14)$$

$$U_z = U_{z,s}\cos(\delta) - U_{x,s}\sin(\delta) \quad (15)$$

$$U_{hor} = \sqrt{U_x^2 + U_y^2} \quad (16)$$

$$\gamma = \arctan\left(\frac{U_y}{U_x}\right) \quad (17)$$

$$\beta = \arctan\left(\frac{U_z}{U_{hor}}\right) \quad (18)$$

3.2. Inverse transformation

The mathematical expressions of the inverse transformation are:

$$U_x = U_{hor} cos(\gamma) \quad (19)$$

$$U_y = U_{hor}\sin(\gamma) \quad (20)$$

$$U_z = U_{hor}\tan(\beta) \quad (21)$$

$$U_{x,s} = U_x\cos(\delta) - U_z\sin(\delta) \quad (22)$$

$$U_{y,s} = U_y \quad (23)$$

$$U_{z,s} = U_x\sin(\delta) + U_z\cos(\delta) \quad (24)$$

$$U = \sqrt{U_{x,s}^2 + U_{y,s}^2 + U_{z,s}^2} \quad (25)$$

$$U_\alpha = \sqrt{U_{y,s}^2 + U_{z,s}^2} \quad (26)$$

$$\alpha = \arctan\left(\frac{U_\alpha}{U_{x,s}}\right) \quad (27)$$

$$U_{z,s} > 0 : \theta = \arctan\left(\frac{U_{y,s}}{U_{z,s}}\right) - \phi \quad (28)$$

$$U_{z,s} \leq 0 : \theta = \arctan\left(\frac{U_{y,s}}{U_{z,s}}\right) - \phi + \pi \quad (29)$$

$$V_1 = U(k_1\cos(\alpha) - k_2\sin(\alpha)\cos(\theta)) \quad (30)$$

$$V_2 = U\left(k_1\cos(\alpha) - k_2\sin(\alpha)\cos(\theta - \frac{2\pi}{3})\right) \quad (31)$$

$$V_3 = U\left(k_1\cos(\alpha) - k_2\sin(\alpha)\cos(\theta - \frac{4\pi}{3})\right) \quad (32)$$

Wind Energ. 0000; **00**:1–21 © 0000 John Wiley & Sons, Ltd.
DOI: 10.1002/we
Prepared using weauth.cls

3.3. Post-calibration of measurements

Knowledge about the conversion algorithm is generally not necessary for the calibration and normal use of a spinner anemometer. It becomes necessary when the user needs to correct measurements taken with a calibration set into the conversion box ($k_{1,d}$, $k_{2,d}$) to different calibration constants (figure 5). The default calibration values are corrected to the new values by use of the correction factors

$$F_1 = \frac{k_1}{k_{1,d}}, \tag{33}$$

$$F_2 = \frac{k_2}{k_{2,d}}, \tag{34}$$

which relates default values to the new values.

The calibration for angular measurements (step 4) provides the ratio

$$F_\alpha = \frac{k_\alpha}{k_{\alpha,d}} = \frac{k_2/k_1}{k_{2,d}/k_{1,d}} = \frac{F_2}{F_1}, \tag{35}$$

used to calibrate inflow angle measurements. When F_1 is calculated (step 5) with the method described in this article, the value of F_2 will be adjusted to keep the correct ratio.

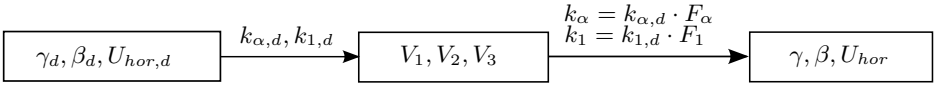

Figure 5. Application of correction factors to measurements taken with default calibration constants

4. CALIBRATION METHOD FOR WIND SPEED MEASUREMENTS

The objective of the wind speed calibration is to find a single value of k_1 that makes the spinner anemometer wind speed (U_{hor}) equal to the free wind speed (U_{mm}) in stopped conditions of the wind turbine. U_{hor} represents the wind speed at the rotor center as if the turbine was not present, since it is a value calibrated to the free wind speed. If the calibration for angular measurements has been made and inserted into the conversion box then the relation U_{mm} to U_{hor} is linear.

Three methods have been developed to calculate the value of the calibration constants – one based on CFD calculations and two based on measurements. When using measurements, the calibration constants are initially set in the spinner anemometer conversion box to default values (for example $k_{1,d} = 1$ and $k_{2,d} = 1$). Based on measurements taken with default constants, the method gives the correction factor F_1 which is then used to correct the default calibration constant $k_{1,d}$ to $k_1 = F_1 k_{1,d}$ [5].

It is important to note that U_{hor} is not the wind speed at the spinner. The actual wind speed at the spinner will be lower than U_{hor} at the front part of the spinner and it will be higher than U_{hor} on the sides of the spinner and between the blades.

U_{hor} is lower than the free wind speed when the turbine is operating due to the rotor induction. To calculate the free wind speed during operation of the wind turbine, the spinner anemometer wind speed U_{hor} must be corrected by use of the NTF (Nacelle Transfer Function, as defined in the standard IEC 61400-12-2 [11]).

The induction is taken into account with the NTF only, and not with k_1. In other words, k_1 only accounts for the spinner and blade root shapes and mounting positions of the sonic sensors.

Table II explains in the first two rows the calculation steps to go from default to calibrated values, and in the third and last row how to go from calibrated value to free wind speed. The present article, however, focuses on the calibration of the spinner anemometer k_1 constant.

From	Action	To
$U_{hor,d}$	Application of F_α (determined in [5])	$U_{hor,d,c}$
$U_{hor,d,c}$	Determination and application of F_1 (chapters 5.4, 5.5, 5.6)	U_{hor}
U_{hor}	Determination and application of the NTF (IEC 61400-12-2, [11])	$U_{hor,free}$

Table II. Calculation steps to convert default values to calibrated values, and finally to free wind speed.

4.1. Application of k_α calibration

The application of the calibration k_α has little effect on the wind velocity component along the shaft axis, while it has a large influence on the angular measurements, as found in [5]. Correcting the measurements to the correct value of k_α gives the important simplification that the relationship between the free reference wind speed and the spinner anemometer wind speed become linear. It is therefore recommended to set the correct k_α value in the spinner anemometer conversion box as soon as it is known. If not set, measurements have to be post-calibrated with the method explained in section 3.3 and [5]. As explained in [5] the post calibration of averaged measurements will introduce an error.

4.2. Calculation of the calibration correction factor F_1

As derived in [5] and summarized in section 3, the calibration factor F_1 is defined as

$$F_1 = \frac{k_1}{k_{1,d}} = \frac{U_d}{U}\frac{\cos(\alpha_d)}{\cos(\alpha)}, \tag{36}$$

where U_d is the magnitude of the wind velocity measured by the non calibrated spinner anemometer, and U is the magnitude of the wind velocity used as a reference for the calibration.

When the measurements of the spinner anemometer have been corrected with F_α, we can neglect the cosine ratio, since $\alpha = \alpha_d$ (the value of the measured inflow angle is correct). This is also the case when the correct $k_\alpha = k_2/k_1$ was set in the conversion box at the time when the measurements were acquired, or the measurements have been corrected with the procedure schematized in figure 5.

The calibration test is performed using the natural wind. The reference wind speed U shall be measured at hub height at a distance upstream of the wind turbine according to [12]. U can be measured with a 3D sonic anemometer or with a specifically designed cup anemometer that measures the vector wind speed rather than the horizontal velocity component. Most of the cup anemometers available on the market are however designed to measure the horizontal component of U. Therefore, under the assumption that the flow inclination at the spinner is equal to the flow inclination at the met-mast we can turn equation 36 into

$$F_1 = \frac{U_{hor,d,c}}{U_{mm}}, \tag{37}$$

so that we compare the horizontal components, instead of the modulus of the wind vectors.

Wind Energ. 0000; **00**:1–21 © 0000 John Wiley & Sons, Ltd.
DOI: 10.1002/we
Prepared using weauth.cls

5. APPLICATION OF THE CALIBRATION METHOD ON A SPECIFIC WIND TURBINE SPINNER ANEMOMETER

A spinner anemometer was mounted on a Nordtank 500 kW wind turbine located at DTU Risø Campus test site, approximately 6 km north of Roskilde, Denmark. The wind turbine has been used for many years for research and educational purposes and is very well instrumented (see description of the site and of the instrumentation in [7]).

Three methods to calibrate the k_1 constants are presented here: for Method 1 the wind turbine is stopped, for Method 2 the wind turbine is in operation, while Method 3 is based on CFD simulation of the stopped rotor.

According to the definition of k_1 (equal to the ratio between the spinner anemometer horizontal wind speed and the free horizontal wind speed in a condition of zero induction) the correct method to determine k_1 is Method 1, which uses a stopped turbine. The drawback of this method is that it requires the wind turbine to be stopped for several hours in good wind conditions, which is generally not acceptable by the wind turbine owner. Therefore we investigated the possibility of determining the calibration constant using measurements during operation of the wind turbine (Method 2) and CFD simulation of the stopped turbine (Method 3). The following subsections describe the instrument set-up, data selection, as well as present an analysis of the three methods.

5.1. Spinner anemometer mounting evaluation

Figure 6 shows the spinner of the Nordtank turbine and two of its sonic sensors. Figure 6 is an overlay of three photos taken from ground level during rotation of the rotor in a way that each photo shows one of the 3 sensors when it is clearly visible on the side of the spinner. The sides of the spinner were used as reference to align the photos. Due to the height of the wind turbine, in order to obtain a good resolution of the photo it was necessary to use a digital camera with a 300 mm zoom optic (12 Megapixel, 18 mm x 24 mm CCD sensor). The camera was standing on a tripod at ground level under the spinner, 1.8 m from the tower.

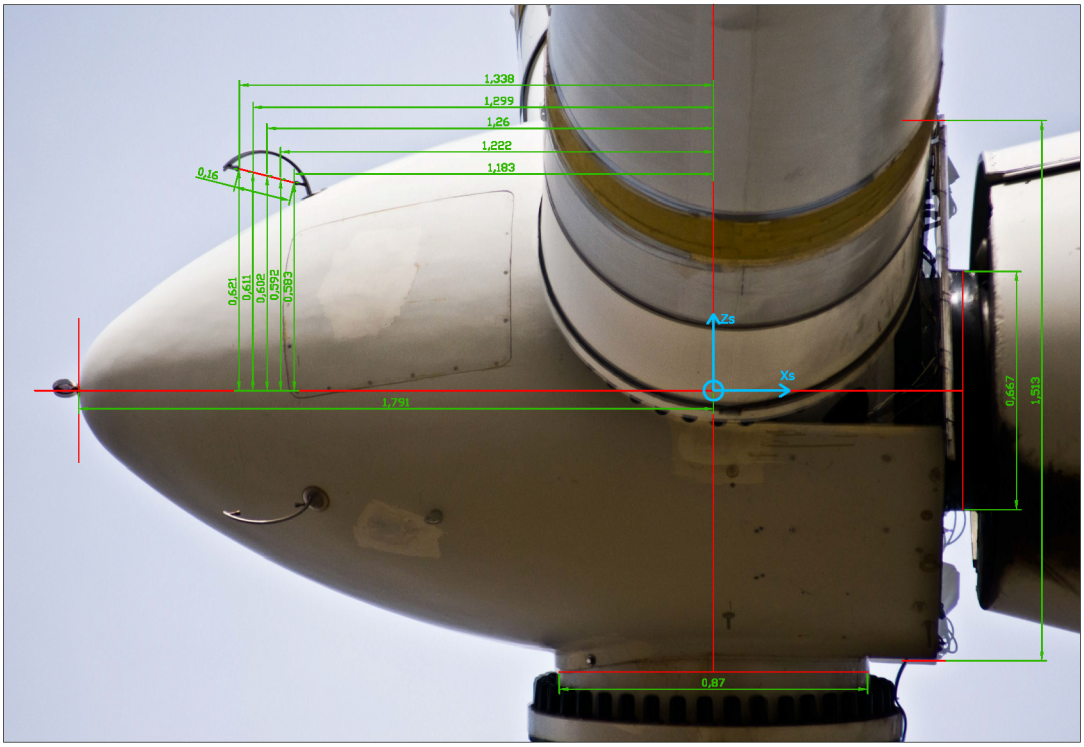

Figure 6. Overlay of 3 photos of the spinner anemometer mounted on the Nordtank 500 kW wind turbine which allows a comparison of the position of the three sonic sensors. The short read line in the sensor path indicates the mean sensor path. The green dimensions show the coordinates of the five points along the sensor path used in the CFD simulation.
The points of sensor 1 are numbered 1 to 5 going from left to right. Table IV gives the coordinate values of each point.

The purpose of the photos was to both determine the absolute position of the sensor paths to define the geometry for the CFD calculations, and verify the relative accuracy of the mounting of the sonic sensors. We scaled the photos to a known dimension of the spinner to be able to measure the position of the sensor path.

In figure 6 the red line drawn in the sonic sensor path (which is 160 millimetres long) indicates the mean path in which the wind velocity components V_1, V_2, V_3 are measured. The CFD results (section 5.6) were extracted in five points along this line.

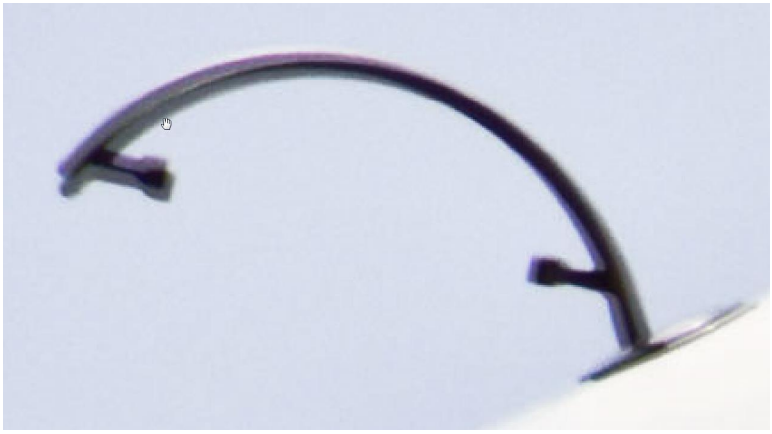

Figure 7. Zoomed in view of the overlay of figure 6 to highlight the relative position of the three sonic sensors.

The deviations between the three sonic sensors show a variation of about 1.8° in the sonic sensor path angle and about 5 mm in longitudinal direction (figure 7). For simplicity in the CFD simulation, we considered that all the sensors were mounted in the exact same position. However, this photographic method could be used to determine the uncertainty in the wind speed measurements due to mounting tolerances and spinner geometry imperfections. The impact of such geometric deviations has not been investigated in detail here because the spinner anemometer was internally calibrated (step 3 of the calibration procedure in figure 2) to compensate for the geometric imperfections. As described in [8], the internal calibration ensures that the three sensors measure the same average wind speed over one rotation.

5.2. Free wind measurement

The met-mast was positioned at 2.5 rotor diameters in a westerly direction with respect to the wind turbine (283°). The measurement of wind speeds at hub height was used to calibrate the spinner anemometer wind speed measurements. The reference instrument was a Risø P2546 cup anemometer mounted on a boom perpendicular to the main wind direction, calibrated in a MEASNET compliant wind tunnel.

The wind direction was measured with a 3D sonic anemometer placed on a second boom 2 m below the cup anemometer, which was not calibrated for wind speed measurements. The valid wind direction sector was $283^\circ \pm 45^\circ$ (238° to 328°). Temperature was measured at the met-mast at hub-height.

5.3. Data selection

The measurement system was active on the wind turbine and met-mast since January 2012. Useful measurements for the present analysis were found in three different measurement periods, A, B, C, see table III. Periods A and B were filtered for measurements during operation of the wind turbine, while period C for measurements during stopped condition due to various reasons.

Period	Turbine condition	Date span	10 minute averages	Calibration set in the conversion box
A	Operation	7/12/2012 - 01/02/2013	525	$k_1 = 1$, $k_2 = 1$
B	Operation	24/05/2014 - 30/06/2014	883	$k_1 = 0.703$, $k_2 = 0.500$
C	Stopped	01/01/2013 - 23/05/2014	353	$k_1 = 1$, $k_2 = 1$

Table III. Calculation steps to convert default values to calibrated values, and finally to free wind speed.

The selection of the measurement periods were made to present broad range of wind speed values. The reason for having three periods instead of two, is that the calibration settings of the spinner anemometer were changed during the

Wind Energ. 0000; **00**:1–21 © 0000 John Wiley & Sons, Ltd.
DOI: 10.1002/we
Prepared using weauth.cls

measurement campaign (in date 23/05/2014) from $k_{1,d} = 1$, $k_{2,d} = 1$ to $k_1 = 0.703$, and $k_2 = 0.500$ (which makes $k_\alpha = k_2/k_1 = 0.711$, found in [5]). Having the correct k_α set in the spinner anemometer conversion box allows for a much easier use of the measurements present in the database. It would not make sense to merge data acquired with different calibration settings. Therefore the measurements of periods A were corrected to the same k_1 and k_2 of period B (using the inverse and direct transformation in chapter 3.3) and only then merged with period B. This merge resulted in 1408 10 minute averages where the met-mast wind speed U_{mm} ranged from 3.6 m/s to 19 m/s.

Measurements of all periods were filtered for temperature larger than 1°C to avoid rime and icing on the cup anemometer. Faulty mast wind speed measurements were removed by deleting the 10 minute data sets where U_{mm} was larger than 50 m/s.

The control system on the turbine reports a status signal of the generator (on-line/of-line) and status of the blade tip brakes (released/retracted). In order to avoid the period of time where the turbine was available but not producing due to low wind speeds, the measurements during operation were obtained by filtering for electrical power output larger than 1 kW.

Measurements during stopped and idling conditions (period C) were obtained by filtering for generator rotations per minute smaller than 20. The data set included measurements from when the wind turbine was stopped for faults, maintenance, or cut-outs. The met-mast wind speed U_{mm} span was from 1 m/s to 27 m/s. The yaw misalignment in stopped conditions never exceeded 40°.

5.4. Calibration of F_1, method 1: comparison with met-mast during stopped conditions

As introduced previously, the scope of the calibration is to find the value of k_1 that makes the spinner anemometer wind speed measurements (U_d) equal to the free wind speed at the rotor center (U) in stopped conditions. Based on measurements taken with default $k_{1,d}$, $k_{2,d}$ constants, the calibration method gives the correction factor F_1 which is then used to correct the default calibration constant $k_{1,d}$ to $k_1 = F_1 k_{1,d}$ [5].

Measurements of horizontal wind speed by the spinner anemometer ($U_{hor,d,c}$), as a function of met-mast horizontal wind speed (U_{mm}), are shown in figure 8. Since the turbine was stopped (data set C), there is no rotor induction effect, and the correction factor F_1 is expected to be independent of the wind speed. This assumption is verified in figure 9, where F_1 is calculated with equation 37.

There is some increased scatter at low wind speeds (below 5 m/s), due to the lower correlation between the met-mast and spinner anemometer. The reason for the high scatter at wind speed lower than 5 m/s seen in figure 9 is that at low wind speeds the correlation between the wind speeds measured at distant locations in space is reduced. This might also be seen by plotting the ratio between two cup anemometers mounted on two met-masts with a horizontal displacement similar to the one between spinner anemometer and met-mast of the present experiment.

The average value of $F_1 = 0.711$ was calculated for wind speeds above 5 m/s, which resulted in the standard deviation of F_1 lower than 2.5% while still keeping 42% of the measurements (149 out of 353). The statistical uncertainty ($\sigma/\sqrt{N}$, where N is the number of samples and σ is the standard deviation) of the mean value is less than 0.002. Since $k_{1,d} = 1$, then $k_1 = 0.711$.

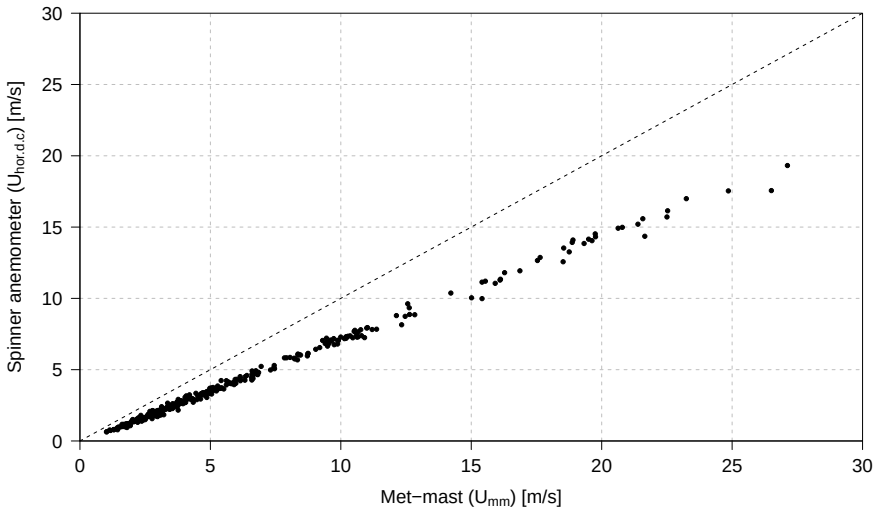

Figure 8. Non calibrated horizontal wind speed by the spinner anemometer as a function of met-mast horizontal wind speed (period C, stopped condition). Black points are 10 minute averages. Dashed black diagonal line is 1:1.

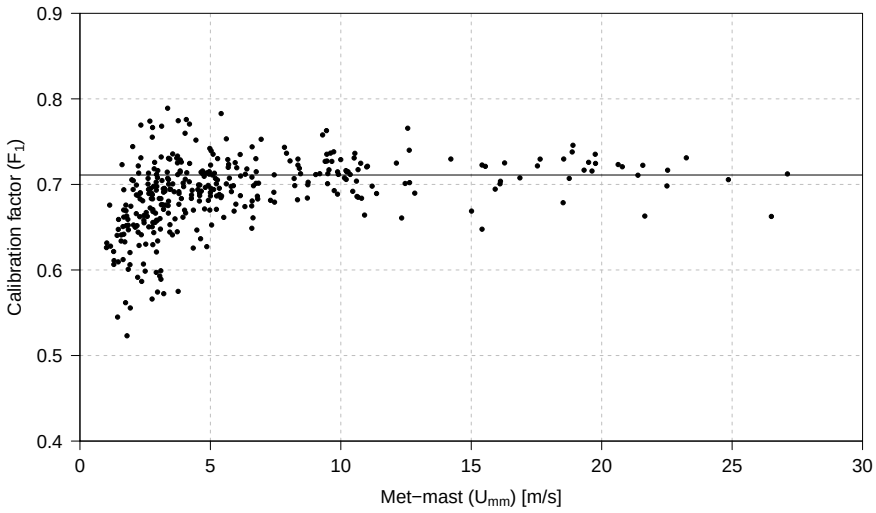

Figure 9. F_1 correction factor as a function of met-mast wind speed (period C, stopped condition). Black points are 10 minute averages. Horizontal black line is at $F_1 = 0.711$

The measurements during stopped conditions calibrated with $F_\alpha = 0.714$ and $F_1 = 0.711$ ($F_2 = F_\alpha F_1 = 0.508$) are shown in figure 10. In the same figure the 1:1 relationship between spinner anemometer measurements and met-mast measurements confirm a correct calibration of F_1 and absence of rotor induction.

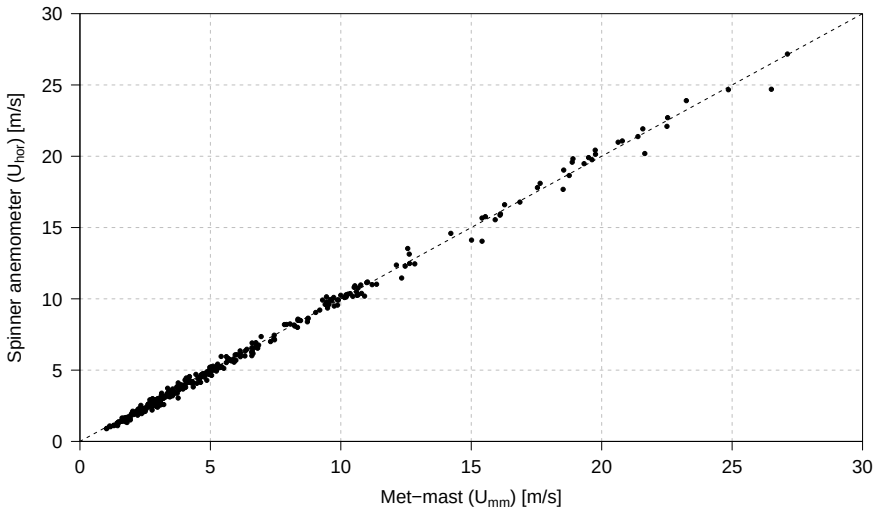

Figure 10. Calibrated horizontal wind speed by the spinner anemometer as function of met-mast horizontal wind speed (period C, stopped condition). Dashed black diagonal line is 1:1.

Wind Energ. 0000; **00**:1–21 © 0000 John Wiley & Sons, Ltd.
DOI: 10.1002/we
Prepared using weauth.cls

5.5. Calibration of F_1, method 2: comparison with met-mast at high wind speeds

This second method to determine F_1 uses measurements during operation of the wind turbine (figure 11).

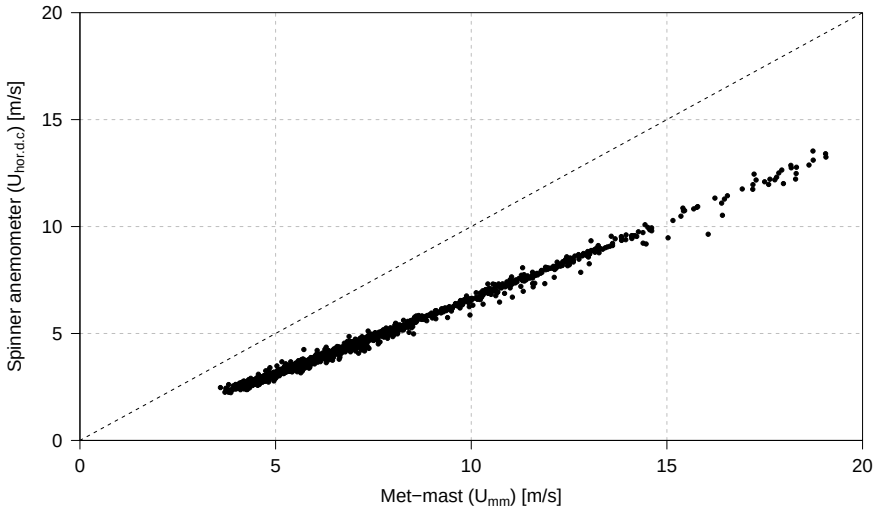

Figure 11. Non calibrated horizontal wind speed by the spinner anemometer as a function of met-mast horizontal wind speed (merge of period A and B, during operation). Dashed black diagonal line is 1:1.

During operation however, the rotor induction reduces the wind speed at the rotor plane with respect to the free wind speed, introducing a significant error in the calculation of F_1. This slow down is small when the turbine is operating at high wind speeds, with a low power coefficient, as seen in [8] and [9], where the induction was found to be smaller than 1% above 17 m/s, for a pitch regulated Vestas V80 wind turbine.

A set of F_1 values was determined from the measurements with equation 37 and plotted as a function of wind speed (figure 12).

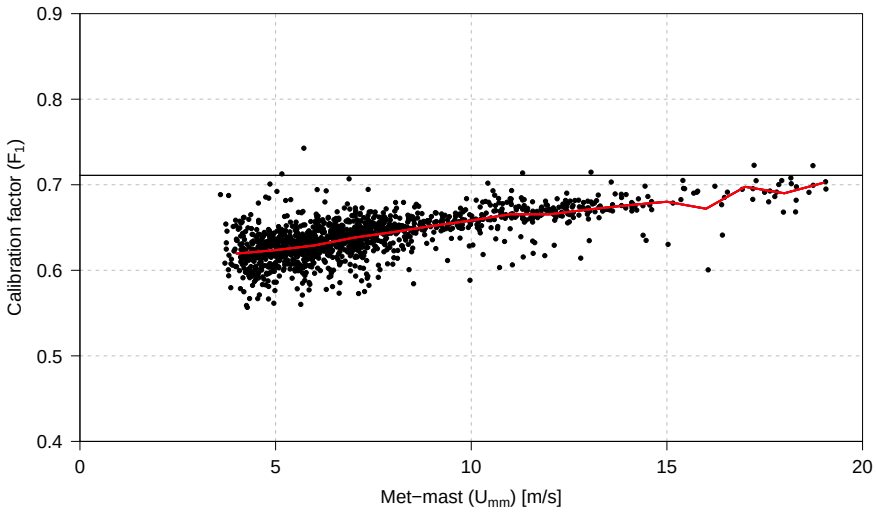

Figure 12. F_1 correction factor as a function of met-mast wind speed, disturbed by the rotor induction during operation of the wind turbine (data set A and B). The black horizontal line at $F_1 = 0.711$ shows the calibration result obtained with method 1 (stopped condition). Black points are 10 minute averages. Red line is 1 m/s bin average.

The red line is a bin average with 1 m/s bin size, centered at integer wind speeds. The horizontal black line shows the value of F_1 found for stopped conditions (section 5.4). As expected, the red line tends asymptotically to the value of F_1 calculated for the stopped rotor (method 1) shown with a horizontal black line. There were unfortunately no measurements

between 18 m/s and 25 m/s. It is not possible to determine a value of F_1 for an induction free condition during operation for the measured data (the red line does not seem to reach an asymptotic value, and increases with the wind speed as a result of the induction decreasing).

The measurements of the period during operation calibrated with $F_\alpha = 0.714$ (found in [5]) and $F_1 = 0.711$ (found in section 5.4 for a stopped rotor) are shown in figure 13 as a function of the met-mast wind speed.

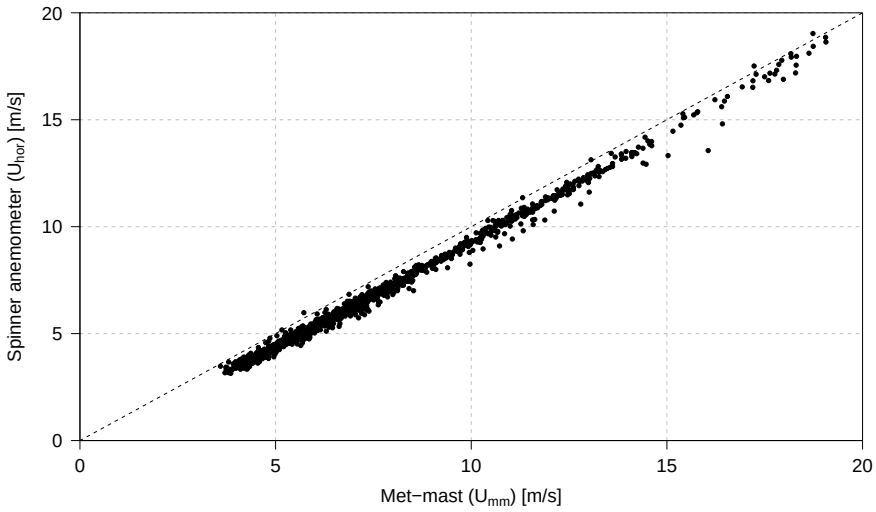

Figure 13. Calibrated horizontal wind speed by the spinner anemometer as a function of met-mast horizontal wind speed (merge of period A and B, during operation). The deviation from the 1:1 dashed line is due to the rotor induction, that makes the wind speed at the turbine lower than the wind speed at the met-mast. This deviation will be accounted for with the NTF, see chapter 6.

5.6. Calibration of F_1, method 3: CFD simulation

Calibration method 3 used CFD for the determination of k_1 for a stopped condition of the wind turbine. The flow field around the turbine was modeled using the EllipSys3D flow solver [16] [17] [18] [19], which solved the incompressible Reynolds-Averaged Navier-Stokes (RANS) equations using the finite volume method in general curvilinear coordinates in a collocated grid arrangement to facilitate complex mesh geometries.

In all simulations, the EllipSys3D code was used in steady state mode, running local time stepping towards a steady state solution. Furthermore, the coupled momentum and pressure-correction equations were solved using the SIMPLE [20] algorithm while the convective terms were discretized using the QUICK [21] scheme.

In the simulations all three blades, spinner and nacelle were modeled according to the actual geometry of the turbine, while the tower was omitted. The total number of cells in the domain was 14 million cells. A grid independence study was conducted and so-called mixed order extrapolation was used to compute the numerical error associated with the sonic sensors on the spinner. This study showed that the velocities extracted in the sensor paths had an error associated with them of approximately 2%. To decrease this error a finer mesh would have to be used.

5.6.1. CFD reference system and geometry description

Looking at the spinner from the front, the CFD reference system has the x axis pointing left, the y axis upwards, and the z axis aligned with the shaft axis (positive in the main stream flow direction). Blade 1 is pointing upwards, hence sensor 1 is at the bottom of the spinner, sensor 2 at the top left, and sensor 3 at the top right.

The CFD simulation gives three velocity components (u, v, w, aligned with x_s, y_s, z_s) at each of the five points in each sonic sensor path (red line in figure 6). The coordinates of the points presented in table IV are obtained by measuring from the photo of figure 1, with fifteen points in total. Points P_1 to P_5 belong to sonic sensor 1 (P_5 being the closest to the spinner surface), P_6 to P_{10} to sensor 2, andP_{11} to P_{15} to sensor 3.

Wind Energ. 0000; **00**:1–21 © 0000 John Wiley & Sons, Ltd.
DOI: 10.1002/we
Prepared using weauth.cls

Sensor	Point	x_s [m]	y_s [m]	z_s [m]
Sensor 1	1	0.000	-0.621	-1.338
	2	0.000	-0.611	-1.299
	3	0.000	-0.602	-1.260
	4	0.000	-0.592	-1.222
	5	0.000	-0.583	-1.183
Sensor 2	6	0.538	0.310	-1.338
	7	0.529	0.305	-1.299
	8	0.521	0.301	-1.260
	9	0.513	0.296	-1.222
	10	0.505	0.291	-1.183
Sensor 3	11	-0.538	0.310	-1.338
	12	-0.529	0.305	-1.299
	13	-0.521	0.301	-1.260
	14	-0.513	0.296	-1.222
	15	-0.505	0.291	-1.183

Table IV. Coordinates of the points of the sensor paths.

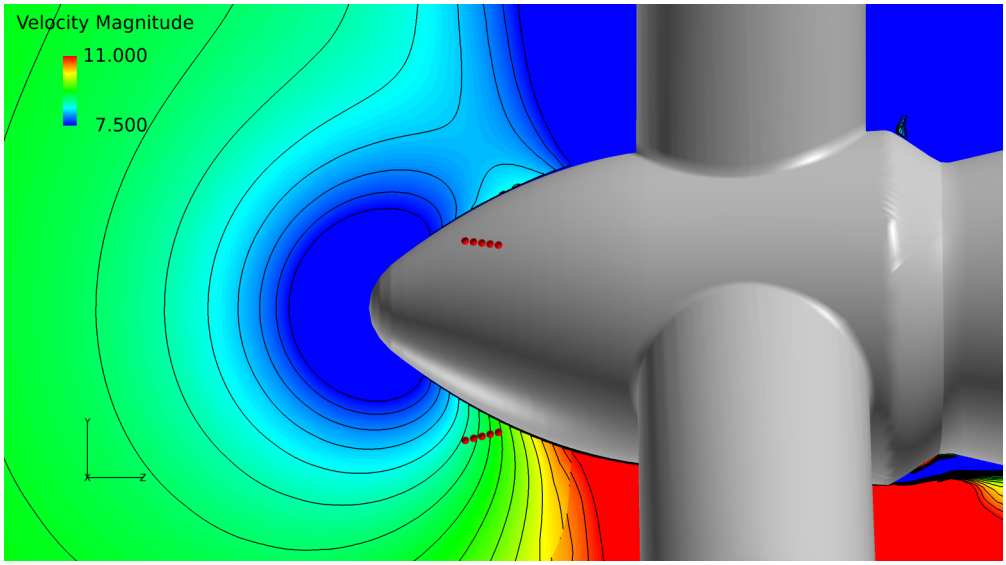

Figure 14. Side view of the wind turbine spinner with one blade vertically upwards. Color represents velocity modulus on a vertical plane in m/s for a free wind speed of 10 m/s. The red dots indicate the position on the sensor path of the CFD results (see figure 6). Low wind speed is found at the stagnation point in front of the spinner and in front of the vertical blade pointing upwards.

5.6.2. Projection along sensor path

The result of the CFD simulation is given as three wind speed components in the global coordinate system. The velocity along the sensor path was calculated as the dot product between the vector velocity $\mathbf{U}(u, v, w)$ and the unit vector of the sensor path $\mathbf{V}(x_s, y_s, z_s)$. The unit vector of the sensor path 1 was calculated as $(\mathbf{r}_{P_5} - \mathbf{r}_{P_1})/(\|\mathbf{r}_{P_5} - \mathbf{r}_{P_1}\|)$.

Figure 15 shows the velocity projected along each sensor path for a free wind speed of 10 m/s. As seen in both figures 14 and 15, the velocity at the point closer to the surface (P_5 for sensor 1) is higher than for the point further from the surface (P_1 for sensor 1). There is full agreement between the three sensors.

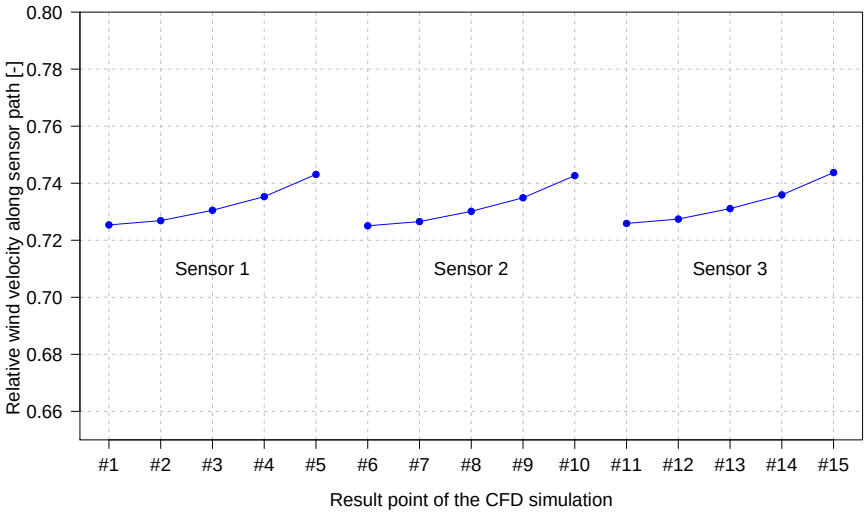

Figure 15. Wind velocity component along the sensor paths in each of the 15 result points in which the CFD results were computed, for a free wind speed of 10 m/s.

5.6.3. Calculation of the k_1 calibration constant from CFD simulations

The flow is simulated for eight wind speeds in the range 4 m/s to 20 m/s, at a flow angle $\alpha = 0$. For this inflow angle, the generic spinner anemometer wind speed relations (equations 1, 2, 3) simplify to equation 38 where the dependency of θ and k_2 vanish. It becomes therefore easy to calculate k_1 using equation 39.

$$V_1 = V_2 = V_3 = U k_1 \tag{38}$$

$$k_1 = \frac{V_1}{U} = \frac{V_2}{U} = \frac{V_3}{U} \tag{39}$$

The geometry of the sonic sensors was not included in the CFD simulation. Therefore the velocity calculated at the points located at the extremes of the sensor path differs from the real velocity, which is influenced by the presence of the sensor heads. Due to this influence the CFD results at the points closer to the sensor heads were neglected (P_1 and P_5 for sensor 1). The velocity along each sensor path was calculated as the average of the three velocities projected along the sensor path (result points P_2, P_3, P_4 for sensor 1).

The calculation of k_1 was repeated for each test wind speed in the range 4 m/s to 24 m/s. The result is shown in figure 16. There is a good agreement between the three sonic sensors. k_1 was expected to be independent of wind speed. However, figure 16 shows a positive trend, with a mean value of 0.7326 and a variation of about $\pm 1\%$. The maximum difference between the values of k_1 calculated for different wind speeds is 0.0226 and the minimum is 0.0095. The increase of k_1 value in the range of wind speeds relevant for power performance measurements (4-16 m/s) is about 1.2%, as seen in figure 16.

Wind Energ. 0000; **00**:1–21 © 0000 John Wiley & Sons, Ltd.
DOI: 10.1002/we
Prepared using weauth.cls

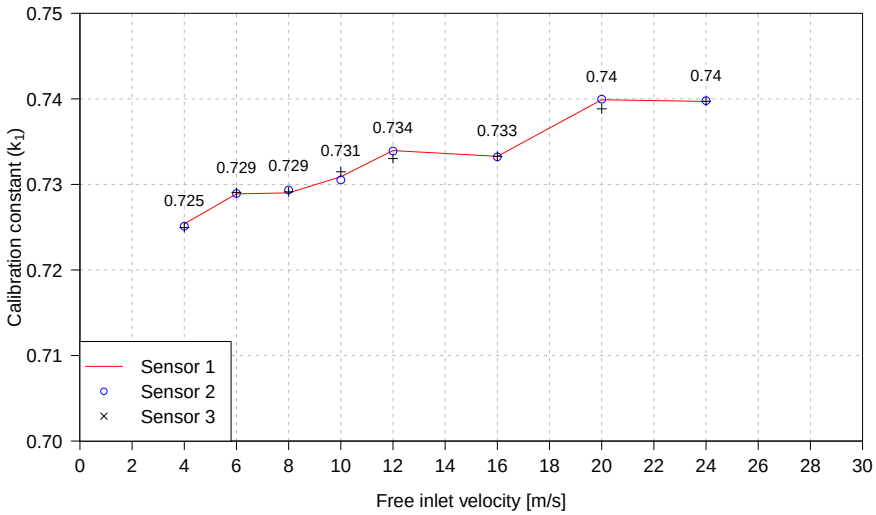

Figure 16. Calibration constant k_1 calculated from CFD simulations at various free wind speeds.
The red line, blue circles and black crosses show the k1 value determined for each of the three sensors.
Numeric values are the mean of the three sensors.

6. NACELLE TRANSFER FUNCTION TO ACCOUNT FOR THE ROTOR INDUCTION

The focus of the analysis is the calibration of the spinner anemometer for wind speed measurements. However this chapter will consider the effect of the induction, and the effect of the application of the NTF (Nacelle Transfer Function) to the measurements during operation (period A and B). A complete description of the method and uncertainty evaluation is available in the report [10]. The induction is defined as the slow down of the wind relative to the free wind as

$$I = \frac{U_{mm} - U_{hor}}{U_{mm}}. \tag{40}$$

As seen in the equation above, the induction is a function of the calibrated spinner anemometer horizontal wind speed U_{hor}. It is not possible to measure the induction if the spinner anemometer is not calibrated for wind speed measurements.

Figure 17 shows the induction at the center of the rotor measured by the calibrated spinner anemometer. At 4 m/s it is 10-15% and gradually decreases for increasing wind speed. At 19 m/s it has not yet reached zero induction.

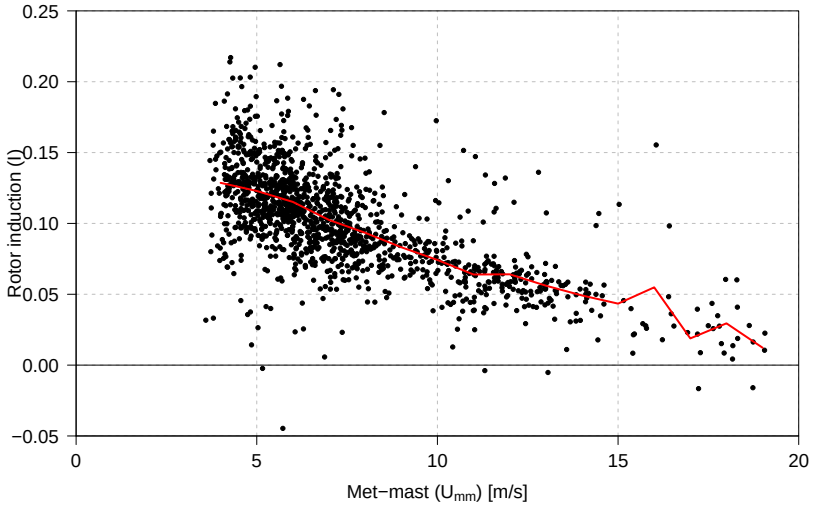

Figure 17. Rotor induction for the stall regulated turbine (during operation).
The horizontal black line is showing the ordinate equal to zero. The red line shows the mean induction for wind speed bins of 1 m/s.

The calibrated horizontal wind speed measured with the spinner anemometer was used to determine the NTF (Nacelle Transfer Function) according to the method described in [11]. The NTF was derived from the measurements of period A and B with the method of bins as shown with a red line in figure 18.

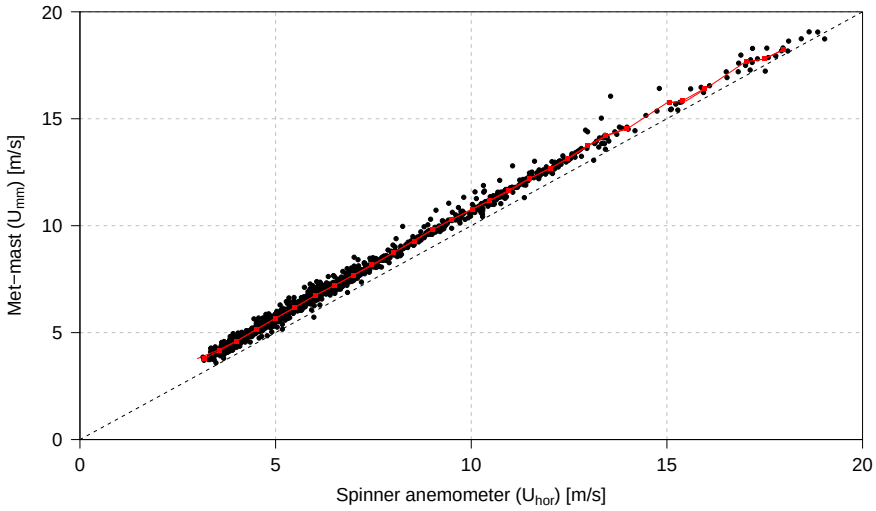

Figure 18. Red dots showing the Nacelle Transfer Function determined as described in IEC61400-12-2 [11]. The NTF is interpolated to adjacent bins at the bins 14.5 m/s and 16.5 m/s because of the amount of 10 minute averages lower than three. The dashed black diagonal line is 1:1.

The measurements of the calibrated spinner anemometer were then converted to free wind speed using the bin values of the NTF ($U_{F,i}$ and $U_{N,i}$) and linear interpolation between bins.

$$U_{free} = \frac{U_{F,i+1} - U_{F,i}}{U_{N,i+1} - U_{N,i}} \cdot (U_{hor} - U_{N,i}) + U_{F,i} \tag{41}$$

A nice linear pattern is shown between calculated free wind speed and measured met-mast wind speed in figure 19.

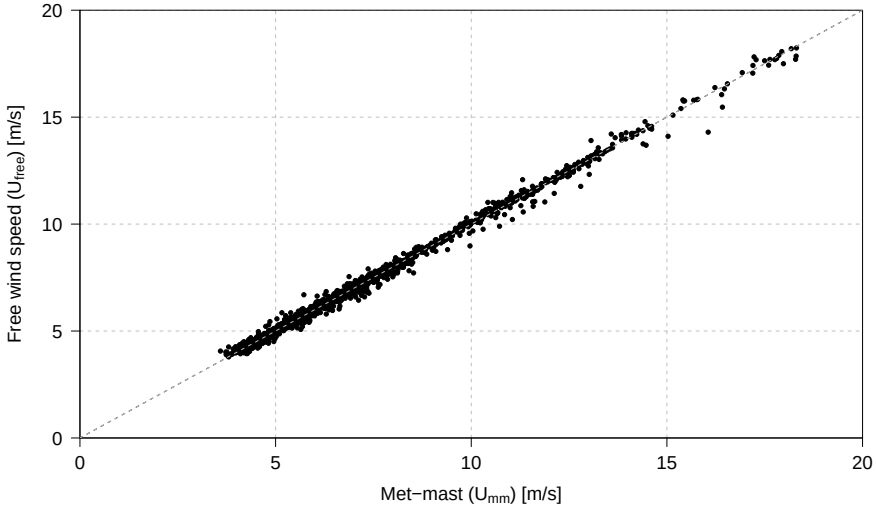

Figure 19. Free wind speed calculated from spinner anemometer measurements corrected with the NTF as a function of met-mast wind speed. The grey dashed line is a 1:1 line.

Wind Energ. 0000; **00**:1–21 © 0000 John Wiley & Sons, Ltd.
DOI: 10.1002/we
Prepared using weauth.cls

7. DISCUSSION

Methods 1 and 2 were based on field measurements, comparing the spinner anemometer wind speed with a met-mast wind speed. 10 minute averages were used to compare the measurements.

Method 1 used measurements of the wind turbine in a stopped condition or while idling. The 353 observations (equivalent to 2.5 days) were acquired over a period of almost 5 months when the wind turbine was stopped for maintenance or other reasons. However, measurements could have been acquired by intentionally stopping the turbine for a number of hours when the wind was at the desired speed and direction, but this was not the case. Still, the results seemed satisfactory.

Method 2 used measurements at moderate wind speeds during operation. As a consequence of the low probability of occurrence of high wind speeds (also combined with the requirements of the valid direction sector), the collection of an appropriate amount of measurements for determination of an induction free k_1 constant was not possible. In the present analysis an observation period of about 3 months was used to collect an amount of measurements of about 10 days, 90% of which the wind speed was below 15 m/s.

Method 3 used a CFD simulation of the velocity in the three sensor paths, in combination with basic equations of the spinner anemometer algorithm to calculate k_1. Different inlet velocities (free wind speed) were used. A summary of the k_1 values found by use of the different methods is shown in figure 20, merging results of figures 9, 12 and 16.

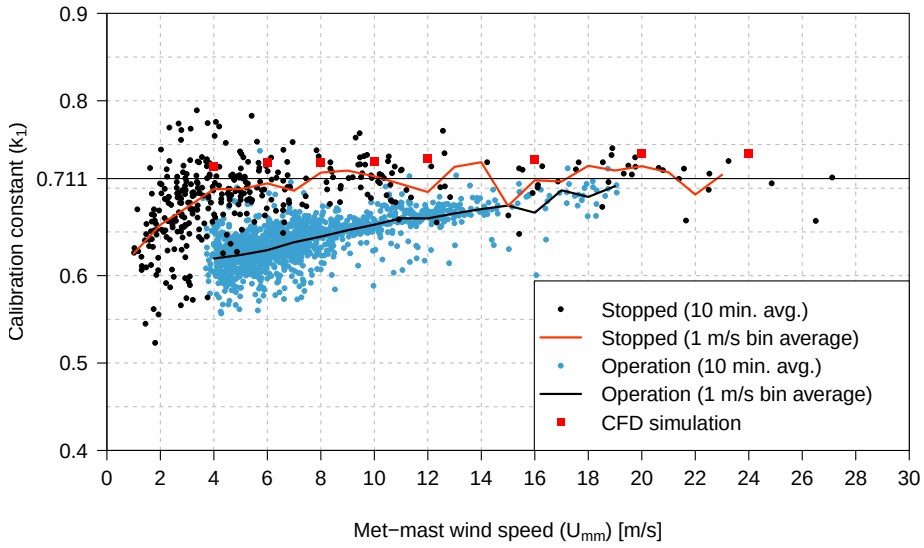

Figure 20. Comparison between the three methods used to calculate k_1. The horizontal black line marks the value of k_1 calculated as average of the vales during stopped condition for wind speed above 5 m/s.

Measurements during operation showed a k_1 that is heavily influenced by induction at the rotor center. For this reason, the calibration must be made in stopped conditions, or during operation ensuring that the induction at very high wind speeds is negligible. This condition of negligible induction was not reached by our stall regulated wind turbine, for the available measurements (up to U_{mm}=19 m/s). A modern pitch regulated turbine however might have a negligible induction at lower wind speeds than a stall regulated turbine, as experienced in [9].

The difference between the CFD results (2.2% to 4.2% overestimation with respect to k_1=0.711) might be due to the uncertainty of the CFD simulation, uncertainty of the cup anemometer on the met-mast, or an underestimation of the wind speed measured by the spinner anemometer in the order of 3%. The spinner anemometer sensors were not in this case calibrated in an accredited wind tunnel as required according to the calibration overview of figure 2. The CFD simulations show a trend of slightly increasing k_1 values for increasing wind speed, about $\pm$1% of mean value. The cause of this trend has not been investigated. The effect is not present in the measurements in stopped condition.

8. CONCLUSIONS

This paper investigated and described three methods to calibrate a spinner anemometer for wind speed measurements, and gave introduction to the consequent use of the NTF (Nacelle Transfer Function) needed to measure the power performance of a wind turbine with the spinner anemometer.

Three methods to determine the k_1 calibration constant for wind speed measurements of a spinner anemometer were presented and compared. Additionally, the use of the nacelle transfer function (NTF) according to IEC 61400-12-2 was introduced to correct measurements to free wind speed.

- Method 1 used a stopped turbine and a comparison between the spinner anemometer wind speed, and the free wind speed measured by the met-mast at hub height.
- Method 2, which was based on the same comparison but during operation of the wind turbine.
- Method 3 used CFD simulation to calculate the wind speeds at the sonic sensor paths, and basic equations of the conversion algorithm to calculate the calibration constant k_1.

According to the definition of k_1 (k_1 is the ratio between spinner anemometer horizontal wind speed and free horizontal wind speed in a condition of zero induction) the correct method to determine k_1 is Method 1, that used a stopped turbine. For Method 1 it was found that the relation between $U_{hor,d}$ and U_{mm} was linear and hence the F_1 correction factor was constant with respect to the free wind speed. The big drawback of this method is that it requires the wind turbine to be stopped for several hours in good wind conditions, which is generally not desirable for the wind turbine owner. Therefore we investigated the possibility of calculating the calibration constant using measurements during operation of the wind turbine (Method 2) and CFD simulation of the stopped turbine (Method 3).

Method 2 was notably influenced by the rotor induction. We tried to identify a range of high wind speeds in which F_1 was stabilizing to an asymptotic value. However, this condition was not met for our stall regulated turbine at wind speeds up to 19 m/s. Method 2 seems to be more applicable on a pitch regulated turbine, where induction decreases more than for a stall regulated turbine due to the pitching of the blades. This will make the F_1 values approach an asymptote.

Method 3, CFD simulation of the stopped turbine, has the obvious advantage of not requiring wind measurements to determine k_1. The method showed a low dependency of k_1 on the wind speed (about 1.2% linear increase from 4 to 16 m/s), and 2.2% to 4.2% difference from the value obtained with method 1. In absence of a free wind speed measurement, this method is appropriate to determine an initial value of the calibration coefficients.

The analysis shows the important simplification of the equations used to calculate k_1 arising from having set the correct k_α value in the spinner anemometer conversion box. Failing to do so means that the full conversion algorithm of sampled data has to be used to calculate back to sonic sensor wind speeds and forth to spinner anemometer wind speed for different k_1 and k_2 values. This was needed in this analysis because data was gathered with k_1 and k_2 values not representing a calibrated k_α value. It is recommended to follow the order of the five steps calibration procedure described in [4].

The calibration of k_1 in addition to determination of the Nacelle Transfer Function (NTF) is needed to measure the nacelle power curve of a wind turbine, ensuring separation between the instrument characteristics and the slow down of the wind due to the rotor induction. It is important to keep the calibration of the spinner anemometer separated from the NTF because the calibration of the spinner anemometer is invariant to control system settings and blade design.

Since the physics of extracting power from the wind is similar between different wind turbines, future research will investigate the possibility of defining a general NTF as a standard correction of the rotor induction. The specificity of the spinner shape and sonic sensors mounting will be accounted by the calibration of the spinner anemometer alone, on each turbine.

ACKNOWLEDGEMENTS

This work was performed as part of an EUDP project iSpin funded by the Danish Energy Agency (J.nr 64012-0107). The authors would like to thank all the people from Vattenfall, Metek, and ROMO Wind for their good collaboration.

REFERENCES

1. Cuerva A, Pedersen TF, Snchez Luengo S, Alamillo Pastor JD, SanzAndrs A, Franchini SA. Theoretical Model on Spinner Anemometry Based on Ultrasonic Paths. *Proceedings of EWEC 2008*. Brussels. 2008.
2. Frandsen S. Nacelle anemometry. *Proceedings of EWEA 2006*. Bruxelles, 2006.
3. Zahle F, Sørensen NN. Characterization of the unsteady flow in the nacelle region of a modern wind turbine. *Wind Energy*, 2011; **14**:271-283.
4. Demurtas G, Pedersen TF. Summary of the steps involved in the calibration of a Spinner anemometer. *DTU Wind Energy report I-0364*. Roskilde, November 2014.
5. Pedersen TF, Demurtas G, Zahle F. Calibration of a spinner anemometer for yaw misalignment measurements. *Wind Energy*, 2014.
6. Pedersen TF, Wagner R, Demurtas G. Wind turbine performance measurements by means of Dynamic Data Analysis. *DTU Wind Energy report*. Roskilde, March 2015.
7. Paulsen US, Wagner R. IMPER: Characterization of the Wind Field over a Large Wind Turbine Rotor-Final report. (Chapter 4: Description of the experimental facility). *DTU Wind Energy report E-0002*. Roskilde, January 2012.
8. Pedersen TF, Demurtas G, Gottschall J, Højstrup J, Nielsen JD, Christiansen W, Weich G, Sommer A, Kristoffersen JR. Improvement of Wind Farm Performance by Means of Spinner Anemometry. Section 2.3: Development of internal calibration method. *DTU Wind Energy report E-0040*. December 2013.
9. Pedersen TF, Demurtas G, Sommer A, Højstrup J. Measurement of rotor centre flow direction and turbulence in wind farm environment. *Torque 2014, Journal of Physics*, Lyngby, June 2014.
10. Demurtas G. Power curve measurement with spinner anemometer according to IEC 61400-12-2. *DTU Wind Energy Report I-0440*. December 2015.
11. IEC 61400-12-2: Power performance of electricity producing wind turbines based on nacelle anemometry. Edition 1, 2012.
12. IEC 61400-12-1: Power performance measurements of electricity producing wind turbines. Edition 3, 2005.
13. Albers A, Jakobi T, Rohden R, Stoltenjohannes J. Influence of meteorological variables on measured wind turbine power curves. *Conference proceedings of EWEC 2007*.
14. Pedersen S. Nacelle anemometry. *EWEA 2006 conference proceedings*. Bruxelles, 2006.
15. Spinner anemometer user manual version 9.27-3. Metek Meteorologische Messtechnik GmBH. Germany, 2012.
16. Jess A. Michelsen. Basis3D - a platform for development of multiblock PDE solvers. *Technical Report AFM 92-05*. Technical University of Denmark, 1992.
17. Jess A. Michelsen. Block structured multigrid solution of 2D and 3D elliptic PDEs. *Technical Report AFM 94-06*. Technical University of Denmark, 1994.
18. Niels N. Srensen. General purpose flow solver applied to flow over hills. *Technical Report Ris-R-827(EN)*. Risø National Laboratory, 1995.
19. Ivanell S, Mikkelsen R, Srensen JN, Henningson D. Validation of methods using EllipSys3D. Technical report, KTH, TRITA-MEK December 2008.
20. Patankar SV, Spalding DB. A calculation procedure for heat, mass and momentum transfer in three-dimensional parabolic flows. *Int. J. Heat Mass Transfer*. **15**:1787-1972, 1972.
21. Leonard PB. A stable and accurate convective modelling procedure based on quadratic upstream interpolation. *Comp. Meth. in Appl. Mech. and Engrng.*. **19**:59-98, 1979.